Tomographic imaging of collagen fiber orientation in human tissue using depth-resolved polarimetry of second-harmonic-generation light

TAKESHI YASUI[1,*], KUNIHIKO SASAKI[1], YOSHIYUKI TOHNO[2] AND TSUTOMU ARAKI[1]

[1]*Graduate School of Engineering Science, Osaka University, Toyonaka, Osaka 560-8531, Japan*
[2]*1st Department of Anatomy, Nara Medical University, Kashihara, Nara 634-8521, Japan*
(*author for correspondence: E-mail: t-yasui@me.es.osaka-u.ac.jp)

Abstract. We propose a nonlinear optical probe method to image the distribution of collagen fiber orientation in human tissue by measuring the polarization of collagen-induced second-harmonic-generation (SHG) light (SHG polarimetry). Depth-resolved SHG polarimetry, with a depth resolution of 14 μm, was used to evaluate the cross-sectional profile of collagen fiber orientation in Achilles tendon and dentin, revealing a characteristic distribution of collagen orientation along the depth direction. We evaluated the two-dimensional (2D) lateral distribution of collagen fiber orientation in back reticular dermis and anklebone by polarization-resolved SHG imaging, and confirmed an appreciable difference in the distribution profiles of the two samples. We further extended the method to a depth-resolved measurement of the three-dimensional (3D) distribution of collagen orientation in anklebone. The proposed system promises to be a powerful tool for *in vivo* measurement of collagen fiber orientation in human tissue.

1. Introduction

Collagen molecules, which form three-dimensional (3D) structural aggregates of successively different sizes (i.e., microfibrils, fibrils, fibers, and bundles), play an important role in determining the morphology and functional properties of tissues and organs as a structural protein. For example, transparency of the cornea is mainly due to polycrystalline lattice of the corneal collagen fibrils whereas inhomogeneous, tubelike structure of scleral fibrils with thin hard shells results in maintaining of the high stiffness and elasticity of the sclera (Han *et al.* 2005). Therefore, there is a considerable need for an optical probe method that can reveal the 3D structure and orientation of collagen fibers and fibrils *in situ* in biological studies and clinical medicine. Recent advances in ultrashort pulse lasers have opened the door to new optical probe methods based on optical nonlinear effects in biological tissue: e.g., two-photon fluorescence (Denk *et al.* 1990),

second-harmonic-generation (SHG) light (Fine and Hansen 1971), third-harmonic-generation (THG) light (Yelin and Silberberg 1999), and coherent anti-Stokes Raman scattering (CARS) light (Zumbusch *et al.* 1999; Hashimoto *et al.* 2000). Such nonlinear optical probes based on multi-photon processes provide unique imaging modality: specific probing power, high spatial resolution, optical sectioning, non-invasion, and deep penetration. Among these probes, the SHG method is an attractive tool for *in vivo* studies of living biological tissues containing collagen molecules. When ultrashort pulse light is incident on collagen-rich tissues, light of half wavelength of the incident light, known as collagen-induced SHG light, is often observed (Roth and Freund 1979). By using this naturally-endogenous SHG process as a contrast mechanism, SHG imaging can clearly visualize structures of collagen fibers and/or fibrils in tissues without additional staining with fluorochrome, and hence it is free from photodamage, photoxicity, or photobleaching. Furthermore, a combination of polarization methods can lead to additional insights. The efficiency of SHG light is sensitive to collagen orientation when the incident light is polarized, and hence polarization measurements of SHG light are effective in probing the collagen orientation in tissues. These SHG probing methods have been successfully applied to various tissue specimens: tendon (Roth and Freund 1979; Stoller *et al.* 2002), dermis (König and Reimann 2003), cornea (Stoller *et al.* 2002; Yeh *et al.* 2002; Han *et al.* 2005), endometrium (Cox *et al.* 2003), and intervertebral disk (Stoller *et al.* 2002). However, few papers have been concerned with human tissue subjects. We have previously proposed polarization-resolved measurements of SHG light in a reflection optics configuration (SHG polarimetry) as a method to extract detailed information of collagen fiber orientation in human tissue (Yasui *et al.* 2004a). We extended the proposed method to two-dimensional (2D) lateral imaging (Yasui *et al.* 2003) and applied it to the characterization of collagen orientation in human dermis (Yasui *et al.* 2004b). Since 3D structures of collagen fibers and fibrils perform various functions in determining morphological and functional properties in tissues and organs, it is necessary to further extend SHG polarimetry in the depth direction to investigate the 3D distribution of collagen fiber orientation in tissue.

In the present paper, we propose depth-resolved SHG polarimetry for the tomography of collagen fiber orientation in human tissue. The penetration power of the proposed method is first investigated for human soft tissue and hard tissue. Using the proposed method, the longitudinal distribution of collagen fiber orientation in human tissue is evaluated in the form of depth-resolved SHG radar graphs. Further, we demonstrate depth-resolved imaging of the 2D lateral distribution of collagen orientation by extending polarization-resolved SHG imaging in the depth direction, which enables reconstructing of the 3D distribution of collagen fiber orientation in human tissue.

2. Experimental setup

The experimental setup for depth-resolved SHG polarimetry is illustrated in Fig. 1. We used an 80-MHz mode-locked Ti:Sapphire laser (Spectra Physics, MaiTai) pumped by a 5-W frequency-doubled Nd:YVO$_4$ laser running at 532 nm. The laser pulse had a duration of 100 fs and an average power of 800 mW at 800 nm. After passing through an optical chopper (OCP, chopping freq. = 3 kHz) and neutral density (ND) filter, ultrashort pulse light from the laser is focused onto the sample with an objective lens [OL, magnification = 20, numerical aperture (NA) = 0.42, working distance = 20 mm], giving an analytical spot of 1.5 μm in diameter and 10 μm in depth in air. Such a relatively low NA value prevents the OL from distorting the polarization of the focus spot of the incident laser light. Although the SHG light induced in the sample mainly propagates in the same direction as the incident light, a portion of the SHG light is backscattered into the tissue, and then collected via the OL. After eliminating the unnecessary laser light with a combination of two harmonic separators (HS, reflected wavelength = 400 nm) and a blue-pass filter (F, pass wavelength = 300–500 nm), the analytical SHG light is detected with a photomultiplier (PMT) and a lock-in-amplifier.

In general, SHG imaging techniques limit the probing volume to a localized focal volume, resulting in confocal-like imaging quality without using a confocal pinhole. However, when applying it to optically thick, turbid medium such as usual human tissue, we have to consider two effects that
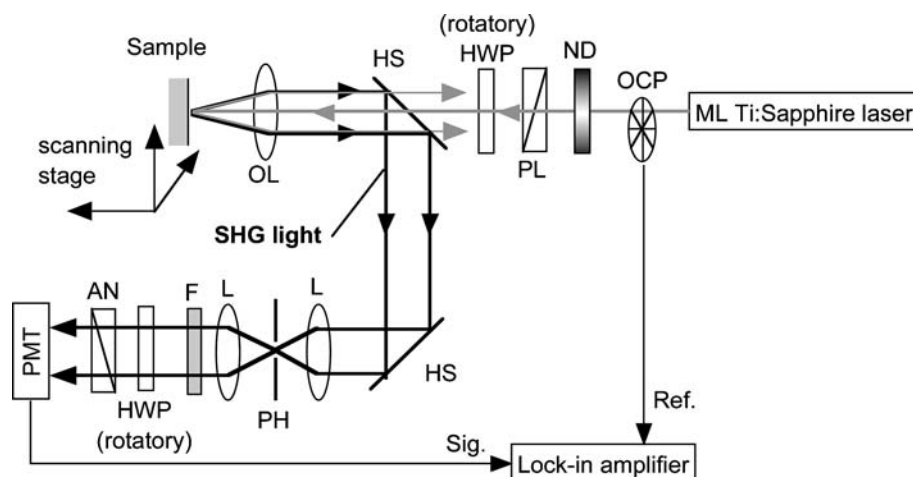

Fig. 1. Experimental setup. OCP: optical chopper; ND: neutral density filter; PL: polarizer; HWP: half-wave plate (rotatory); HS: harmonic separator; OL: objective lens; L: lens; PH: pinhole; F: blue-pass filter; AN: analyzer; PMT: photomultiplier.

may degrade the imaging characteristics: scattering and refractive index mismatching. The imaging characteristics of two-photon microscopy in a turbid medium have been investigated comprehensively (Centonze and White 1998; Dunn *et al.* 2000; Dong *et al.* 2003), and it is reported that the scattering does not significantly affect the two-photon point-spread-function down to a depth of 200 µm (Dong *et al.* 2003). In the present SHG setup with a probing depth of a few 100s µm, it can be consider that the imaging characteristics are hardly affected by the scattering in the same manner as the two-photon microscopy although we have to consider that the SHG is a coherent nonlinear optical process. On the other hand, the refractive index mismatching induces the spherical aberration depending on the imaging depth, which degrades the point-spread-function (Dong *et al.* 2003). This results in a blurred analytical spot when probing deep portions in a thick tissue sample. Hence, deep optical sectioning of the tissue requires a confocal configuration with a detection pinhole, even if the pinhole decreases the SHG signal level. In the present setup, to improve the spatial resolution for depth-resolved measurements, a confocal configuration, comprising a pinhole (PH) and two lenses (L, $f = 50$ mm), is introduced in the SHG optical path. Although a diameter of Airy disk is about 10 µm at the PH position, a PH of 50 µm in diameter is selected by considering a relationship between the achieved spatial resolution and the detected SHG signal level. The resulting depth resolution was 14 µm. Simultaneously, the confocal configuration decreases depolarization effects in the incident laser light and analytical SHG light caused by multiple-scattering in the depth-resolved measurement of a thick tissue sample.

For SHG polarimetry, a polarizer (PL), two half-wave plates (HWP, rotatory), and an analyzer (AN) are inserted in the light path. The polarization of the incident laser light and of the detected SHG light are rotated synchronously, keeping them parallel to each other, by the two mechanically-rotated HWP. Although this rotation procedure is equivalent to the rotation of the sample around the optical axis under fixed polarization optics, it is difficult to coincide the sample rotating axis and the optical axis within the analytical spot, and hence we chose to use a polarization-rotating setup. The distribution of the SHG light intensity is measured with respect to the polarization angle. For the imaging measurement of the SHG light, the sample is scanned by a 3D moving stage.

3. Sample

In this experiment, we used four kinds of human tissue samples rich in collagen. Back reticular dermis (from a cadaver) and Achilles tendon (from a cadaver) were prepared as soft tissue samples. The cadavers were treated

by injecting a mixture of 36% ethanol, 13% glycerin, 6% phenol, and 6% formalin through the femoral artery. After a typical dissection by medical students in an anatomy class at Nara Medical University was carried out, the tendon and skin were resected. The tissue samples were washed with distilled water and then dried in air. We have confirmed that these sample preparation procedures (formalin fixation and air-drying) do not affect the results of SHG polarimetry (Yasui *et al.* 2004b). Two kinds of tendon specimens with different thicknesses (2 mm and 0.3 mm) were prepared by slicing them along the axial direction. The skin was stripped off the cadaver's back and subcutaneous tissue was removed with a scalpel to expose the reticular dermis layer. The exposed reticular dermis was cut into a 44 mm × 55 mm square sheet of 1 mm thickness. As hard tissue samples, we prepared dentin (extracted by a dentist) and anklebone (from a cadaver). The dentin and anklebone were sliced to 1 mm thickness along the tooth axis and 2 mm thickness across the section, respectively, with a tooth/bone cutter. We have previously confirmed using SHG polarimetry that the Achilles tendon, the back reticular dermis, the dentin, and the anklebone possess uniaxial, randomly entangled, crossed biaxial, and parallel-to-crest oriented collagen fibers, respectively (Yasui *et al.* 2004a, b).

4. Results

4.1. PENETRATION POWER OF DEPTH-RESOLVED SHG MEASUREMENT

We first evaluated the penetration power of the depth-resolved SHG measurements for an incident laser power of 25 mW. The analytical laser spot was scanned in the depth direction from the sample surface. The sample specimens examined were the Achilles tendon and the back reticular dermis, as human soft tissue samples, and the dentin as a human hard tissue sample. Figure 2 shows decay curves of SHG light intensity with respect to depth position for the three sample specimens. The depth resolution in the present system was 14 μm, determined from another experiment using a sufficiently thin slice (thickness < 5 μm) of a mouse tendon (not shown). At a depth of 0 μm, the analytical spot was focused on the sample surface. The resulting maximum penetration depths were 300, 150, and 100 μm for the tendon, dermis, and dentin, respectively. These penetration powers can be improved by matching the refractive indices of the sample and the objective lens by using an oil-immersion objective lens. An alternative method is to use a deep-penetrative femtosecond laser with a longer wavelength, such as a mode-locked Cr:Forsterite laser with a center wavelength of 1250 nm. Efforts to improve the penetration power by these two methods are in progress.
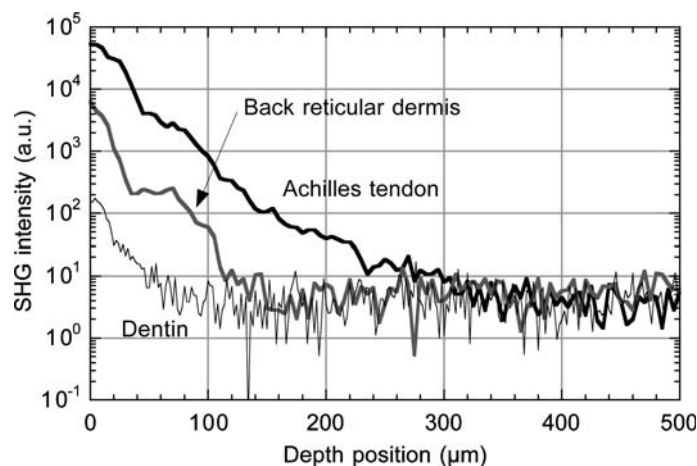
Fig. 2. Decay curves of SHG light intensity with respect to depth position for three different human tissues. The incident laser power and depth resolution are 25 mW and 14 μm, respectively. A depth of 0 μm indicates the analytical spot focused onto the sample surface.

4.2. DEPTH-RESOLVED SHG POLARIMETRY

We next performed depth-resolved SHG polarimetry of a tissue sample with a different collagen orientation along the depth direction, to evaluate the basic performance of this method. We stacked two sliced Achilles tendons (thickness = 0.3 mm) with their collagen orientations perpendicular to each other, as shown in Fig. 3(a). Figure 3(b) shows the resulting SHG radar graph with respect to polarization angle, scanning the analytical spot along the depth direction. Here we refer to 0 (or 180) and 90 (or 270) degrees as horizontal and vertical polarization, respectively. The polarization angle of the major axis and the profile of the SHG radar graph reveal, respectively, the direction of the absolute orientation and the degree of organization of the collagen fibers in the area of the light spot. The gray arrows in each of the plots of Fig. 3(b) indicate the expected direction of collagen orientation. In general, collagen SHG light is output strongly with the same polarization as the incident light when the polarization direction of the incident light is parallel to the longitudinal direction of the collagen fiber (Yasui *et al.* 2004a). However, the SHG light almost disappears if the laser polarization is perpendicular to the collagen orientation. Such sharp polarization sensitivity is due to differences in the $\chi^{(2)}$ tensor components. Hence, the SHG radar graph at 0-μm depth (the surface of the first tendon layer) shows that the collagen fiber was well aligned along the horizontal direction. The profile was rotated about 90 degrees at 350-μm depth, indicating vertical orientation of the collagen fiber in the second layer. Furthermore, a mixed profile of horizontal and vertical orientation was observed
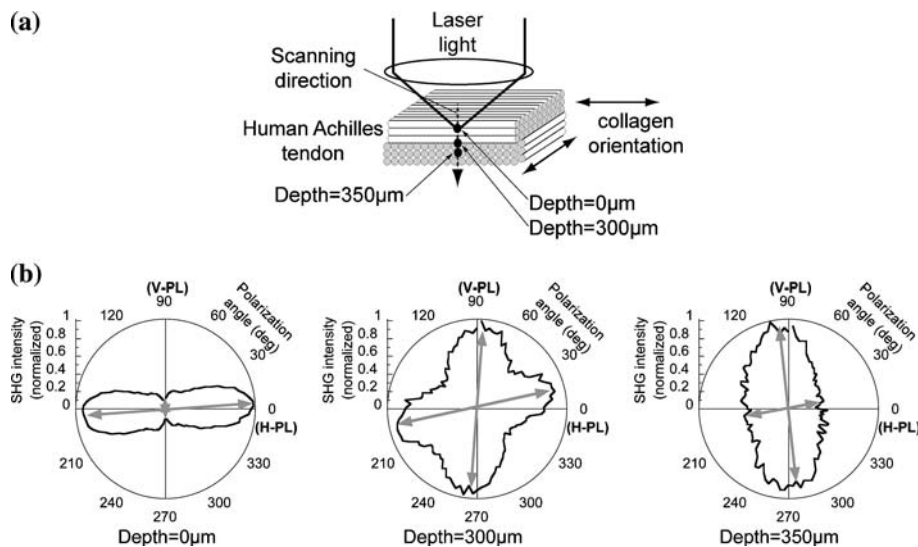
Fig. 3. Basic characteristics of depth-resolved SHG polarimetry. (a) Sample. Two sliced Achilles tendons stacked so that their collagen orientations are perpendicular to each other. (b) Depth-resolved SHG radar graph. The 0, 300, and 350-μm depths indicate that the analytical spot is located on the surface of the first tendon layer, the boundary between the first and the second tendon layers, and the second tendon layer, respectively.

at a depth of 300 μm, which locates the boundary between the first and second tendon layers. These results clearly indicate that the proposed system is effective for the tomographic measurement of collagen orientation in tissue. However, there is an outstanding issue to be addressed in the present system. The profile of the SHG radar graph at 0-μm depth exhibits a node at the origin, whereas no node is observed at 350-μm depth, although the figure-eight profile is characteristic for SHG radar graphs of Achilles tendon with uniaxial collagen orientation (Yasui *et al.* 2004a). This result might imply some depolarization of the incident laser light and the analytical SHG light in the tissue when probing a deep portion of a sample. Such a depolarization effect can be counteracted by using a sharper confocal configuration at the expense of signal efficiency.

We applied depth-resolved SHG polarimetry to the human tissue samples. Figure 4(a) and (b) show the resulting depth-resolved SHG radar graphs of the Achilles tendon (thickness = 2 mm) and the dentin. In these graphs, the horizontal and vertical axes indicate the depth position and polarization angle, respectively. Five SHG radar graphs are also illustrated from the vertical line profiles at five depth positions in the depth-resolved SHG radar graphs. The SHG radar graph in Fig. 4(a) of the Achilles tendon indicates uniaxial collagen orientation in the vertical direction at each depth position. In a previous study, we reported that human Achilles tendon possesses a
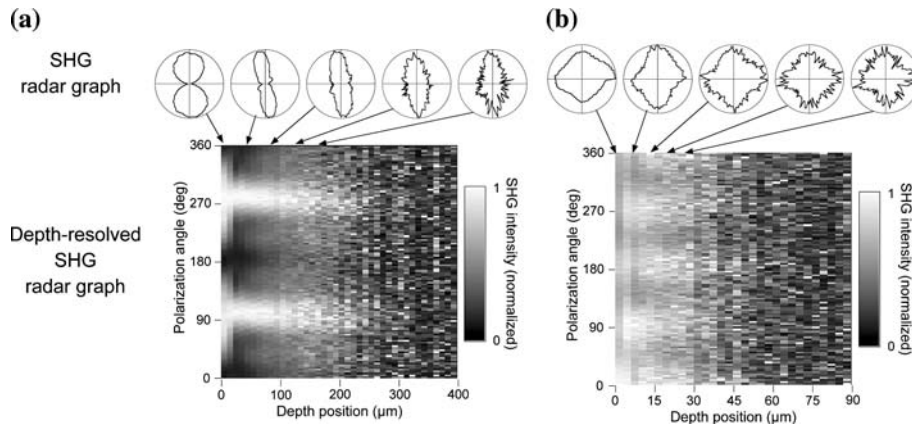
Fig. 4. Depth-resolved SHG radar graphs of human tissues. (a) Human Achilles tendon and (b) human dentin. The 0-µm depth indicates that the analytical spot is focused onto the sample surface. Five SHG radar graphs illustrate a vertical line profile at each depth position in the depth-resolved SHG radar graph.

characteristic 2D lateral distribution of collagen orientation in which the collagen fiber is arranged with a high organization (Yasui *et al.* 2003). From the present results for the longitudinal direction and the previous results for the 2D lateral direction, we conclude that the collagen orientation is arranged with a highly organized three-dimensional distribution. On the other hand, in Fig. 4(b) we observed that a crossed, biaxial orientation of collagen fiber is uniformly distributed along the depth direction in the dentin. We previously confirmed that the 2D lateral distribution of collagen orientation in dentin gradually becomes disordered, from biaxial at the root to random at the crown, depending on the growth lines (Yasui *et al.* 2004a). The present tomographic measurement of the collagen orientation was performed along the depth direction on the same growth line. Differences in the collagen orientation distribution in the longitudinal and 2D lateral directions are interesting from the viewpoint of both the size effect of the measurement region and metabolic effects such as tooth aging. To confirm these differences, further examination of different types of teeth is essential.

4.3. 2D LATERAL DISTRIBUTION OF COLLAGEN ORIENTATION AT SAMPLE SURFACE

We performed polarization-resolved SHG imaging of the 2D lateral distribution of collagen orientation at the sample surface. Figure 5(a) and (b) show, respectively, vertically- and horizontally-polarized SHG images of the anklebone (image size = 3 mm × 3 mm). Although we can clearly observe
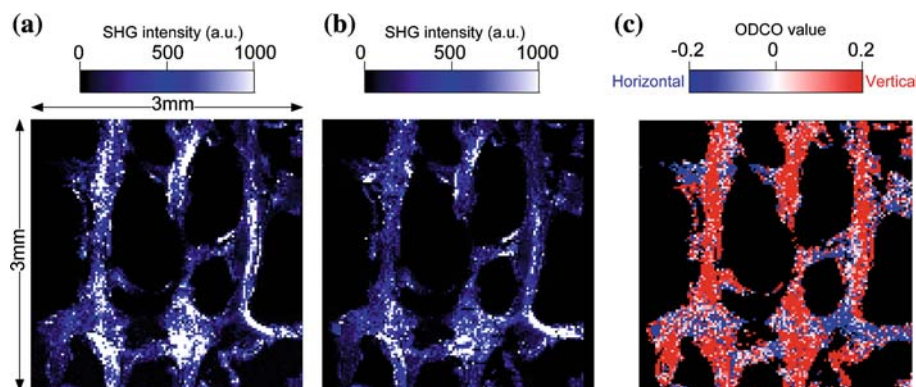
Fig. 5. 2D lateral distribution of collagen fiber orientation at the surface of human anklebone. (a) Verti-cally-polarized SHG image, (b) horizontally-polarized SHG image, (c) ODCO image calculated from the two polarization-resolved SHG images. Image size is 3 mm by 3 mm. The color scale of the ODCO value indicates the direction of collagen orientation: red for vertical, blue for horizontal.

the 2D distribution of SHG light along the crest of the anklebone, it is difficult to recognize the detailed distribution of the collagen orienta-tion from a direct comparison between the two polarization-resolved SHG images. Hence, we define a quantity for the polarization anisotropy of SHG light, the organization degree of the collagen orientation (ODCO), using the following equation:

$$\mathrm{ODCO} = (I_V - I_H)/(I_V + I_H), \tag{1}$$

where I_V and I_H are the vertically- and horizontally-polarized SHG inten-sities, respectively. The collagen orientation is uniaxial for $\mathrm{ODCO} = \pm 1$ and random or biaxial for $\mathrm{ODCO} = 0$. The sign of ODCO gives the dominant direction of the collagen orientation: positive for vertical orientation and negative for horizontal orientation. Figure 5(c) shows the resultant ODCO image of the anklebone. The color scale of the ODCO value indicates the direction of the collagen orientation, with vertical indicated by red and hor-izontal by blue. Here, focusing on the relationship between the structure of the bone crest and the color in the image, we observe that the verti-cally-running crests are largely red while the horizontally-running crests are largely blue. In other words, the anklebone possesses a characteristic 2D lateral distribution of collagen fiber orientation at the surface in which the direction of the collagen orientation is approximately consistent with the bone crest direction. This result is in good agreement with histological find-ings of bone structure (Langton and Njeh 2004).

In the next experiment, the 2D distribution of the collagen orientation angle in the reticular dermis was investigated. For this purpose, we mea-sured six polarization-resolved SHG images at every 30 degrees. Figure 6(a)

shows six polarization-resolved SHG images of 1 mm by 1 mm at 0, 30, 60, 90, 120, and 150 degrees. By comparing these six images, we can determine the polarization angle for each pixel by identifying the image that displays the maximum intensity for that pixel, hence indicating the orientation direction. Figure 6(b) shows the resulting 2D vector map of the orientation angle for the reticular dermis. Even in the 2D distribution, we can confirm the winding of the orientation angle, as indicated by the gray stripe, similar to the 1D distribution of the collagen fiber orientation of the reticular dermis in the previous study (Yasui *et al*. 2004b). The present result is consistent with the histological findings for reticular dermis, in which thickly-growing collagen fibers and bundles run entangled in the tissue.

4.4. DEPTH-RESOLED IMAGING OF 2D LATERAL DISTRIBUTION OF COLLAGEN ORIENTATION

Finally, we performed depth-resolved imaging of the 2D lateral distribution of collagen orientation in the anklebone. For this purpose, we extended
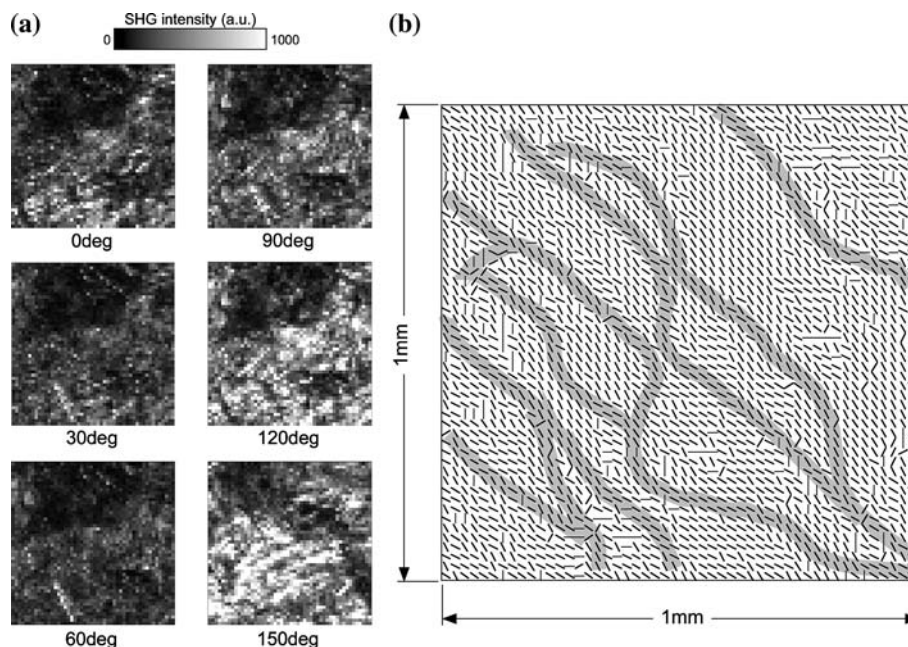

Fig. 6. 2D lateral distribution of collagen fiber orientation at the surface of human back reticular dermis. (a) Polarization-resolved SHG images at 0, 30, 60, 90, 120, and 150 degrees (image size = 1 mm × 1 mm). (b) 2D vector map of orientation angle. The orientation angle for any pixel was determined to be the polarization angle showing the maximum SHG intensity among the six polarization-resolved SHG images.
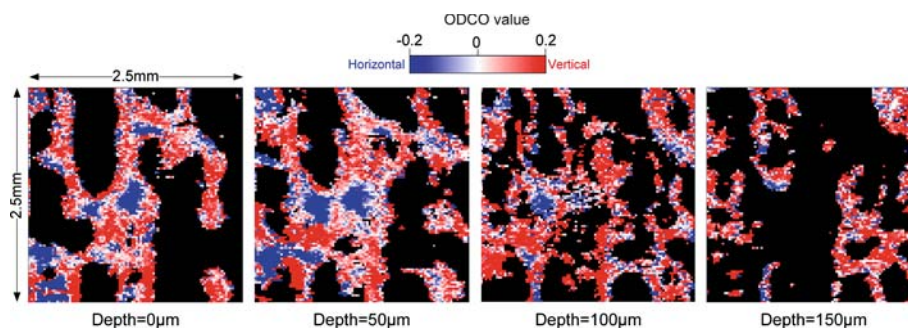
Fig. 7. Depth-resolved ODCO images of 2D lateral distribution of collagen fiber orientation for human anklebone at depths of (a) $0\,\mu$m (sample surface), (b) $50\,\mu$m, (c) $100\,\mu$m, and (d) $150\,\mu$m (image size $= 2.5\,$mm $\times 2.5\,$mm). The color scale of the ODCO value indicates the direction of collagen orientation: red for vertical, blue for horizontal, respectively.

the 2D lateral ODCO imaging along the depth direction. Figure 7 shows 2D lateral ODCO images of the anklebone at depths of $0\,\mu$m (sample surface), 50, 100, and $150\,\mu$m (image size $= 2.5\,$mm $\times 2.5\,$mm). Although there is a lack of image signal at 150-μm depth due to weak SHG light, the 3D structure of the bone crest can be clearly visualized from the four successive ODCO images at each depth. Furthermore, the collagen orientation parallel to the crest direction continuously develops along the depth direction in the same manner as in the 2D lateral direction, the mechanical property of which is adapted to bear a mechanical load in any direction. A combination of such measurements and 3D control of laser polarization angle (Yoshiki *et al.* 2005) could reconstruct the 3D distribution of collagen fiber orientation in human tissue.

5. Conclusions

Depth-resolved SHG polarimetry with a confocal pinhole was proposed as an effective method to probe the tomographic distribution of the collagen fiber orientation in human tissue. A maximum penetration depth of $100\,\mu$m for human hard tissue and 150–$300\,\mu$m for two samples of human soft tissue was achieved, for which the incident laser power and the depth resolution were $25\,$mW and $14\,\mu$m, respectively. We examined the efficacy of the proposed method for the tomography of collagen orientation using first a stacked sample, each of which had a known collagen orientation along the depth direction, and then applied it to human tissue samples. The resulting depth-resolved SHG radar graphs indicate a uniform distribution of the uniaxial orientation and the biaxial orientation along the depth direction for Achilles tendon and dentin, respectively. We also investigated

the 2D lateral distribution of collagen orientation and demonstrated depth-resolved imaging of this distribution based on 2D lateral ODCO imaging calculated from two perpendicularly-polarized SHG images. Back reticular dermis exhibited an entangled structure of collagen fiber at the 2D lateral surface, whereas anklebone possessed a 3D collagen orientation parallel to the bone crest. The proposed system promises to be a powerful tool for *in vivo* monitoring of human tissue collagen, such as dermis or cornea.

Acknowledgements

References

Centonze, V.E. and J.G. White. *Biophys. J.* **75** 2015, 1998.

Cox, G., E. Kable, A. Jones, I. Fraser, F. Manconi and M.D. Gorrell. *J. Struct. Biol.* **141** 53, 2003.

Denk, W., J.H. Strickler and W.W. Webb. *Science* **248** 73, 1990.

Dong, C.-Y., K. Koenig and P. So. *J. Biomed. Opt.* **8** 450, 2003.

Dunn, A.K., V.P. Wallace, M. Coleno, M.W. Berns and B.J. Tromberg. *Appl. Opt.* **39** 1194, 2000.

Fine, S. and W.P. Hansen. *Appl. Opt.* **10** 2350, 1971.

Han, M., G. Giese and J.F. Bille. *Opt. Express* **13** 5791, 2005. http://www.opticsexpress.org/abstract.cfm?URI=OPEX-13-15-5791.

Hashimoto, M., T. Araki and S. Kawata. *Opt. Lett.* **25** 1768, 2000.

König, K. and I. Riemann. *J. Biomed. Opt.* **8** 432, 2003.

Langton, C.M. and C.F. Njeh. In: *The Physical Measurement of Bone*, Institute of Physics Publishing, London, 11, 2004.

Roth, S. and I. Freund. *J. Chem. Phys.* **70** 1637, 1979.

Stoller, P., K.M. Reiser, P.M. Celliers and A.M. Rubenchik. *Biophys. J.* **82** 3330, 2002.

Yasui, T., K. Shimabayashi, Y. Tohno and T. Araki. In: *The 5th Pacific Rim Conference on Lasers and Electro-Optics CLEO, Proc. The 5th Pacific Rim Conference on Lasers and Electro-Optics*, TaiPei, 15–19 December 2003, 361, 2003.

Yasui, T., Y. Tohno and T. Araki. *Appl. Opt.* **43** 2861, 2004a.

Yasui, T., Y. Tohno and T. Araki. *J. Biomed. Opt.* **9** 259, 2004b.

Yeh, A.T., N. Nassif, A. Zoumi and B.J. Tromberg. *Opt. Lett.* **27** 2082, 2002.

Yelin, D. and Y. Silberberg. *Opt. Express* **5** 169, 1999. http://www.opticsexpress.org/abstract.cfm?URI=OPEX-5-8-169.

Yoshiki, K., M. Hashimoto and T. Araki. *Jpn. J. Appl. Phys.* **44** L1066, 2005.

Zumbusch, A., G.R. Holtom and X.S. Xie. *Phys. Rev. Lett.* **82** 4142, 1999.